JPE 18-1-24

https://doi.org/10.6113/JPE.2018.18.1.266
ISSN(Print): 1598-2092 / ISSN(Online): 2093-4718

Research on a New 12-Pulse Step-Up and Step-Down Aviation Auto-Transformer Rectifier

Fan Jiang†, Hong-juan Ge*, Xiao-xu Dong*, and Lu Zhang*

†,*Nanjing University of Aeronautics and Astronautics, Nanjing, China

Abstract

This paper presents a new step-up and step-down multi-pulse auto-transformer rectifier unit (ATRU) topology. This structure can achieve a wide range of output voltages, which solves the problem of auto-transformer output voltage being difficult to regulate. Adding middle taps to the primary winding and reasonably setting the number of auto-transformer windings, constituted two groups of three-phase output voltages with a 30° phase difference. Multi-pulse output DC voltage is obtained after a three-phase output voltage across two rectifier bridges and inter-phase reactor. Thus, the output DC voltage is related to the number and configuration of the auto-transformer winding. In this paper, the relationship between the voltage ratio of the auto-transformer and the ratio of winding, input current and auto-transformer kilovoltampere rating are deduced and validated by simulations. On this basis, the output voltage range is optimized. An experiment on two different voltage ratio principle prototypes was carried out to verify the correctness of the analysis design.

Key words: Auto-transformer, Kilovoltampere rating, Multi-pulse rectifier, Step-up and step-down

I. INTRODUCTION

At present, AC-DC transform power technology such as controlled rectifiers and PWM rectifiers have matured [1]-[4]. However, they have a great influence on power supply system due to the high frequency harmonics caused by high frequency modulation, so it is seldom used in the aircraft power supply system [7], [9], [12], [16], [20]. The AC-DC converter used in the aviation power supply is multi-pulse transformer rectifier. The ATRU has a wide range of applications. It can reduce the volume and weight of a filter unit, and has the advantages of close coupling, small volume, light weight and high efficiency [5]-[8]. Since 1995, domestic and foreign scholars have carried out a series of research on topologies, suppression of harmonic content, kilovoltampere rating and the output voltage regulation of ATRU [9]-[16]. In these studies, research on the output voltage regulation of ATRU is relatively rare.

12-pulse and 18-pulse ATRUs based on wye connections and delta connections were studied in [17], which proposed that output voltage regulation was achieved by changing the connecting position of the secondary winding of auto-transformer. The relation of the voltage of each winding was deduced and an experimental analysis was carried out on an 18-pulse ATRU. However, there are relatively few analysis of the input current harmonic, kilovoltampere rating and other parameters. In [18], the auto-transformer structure, input current, kilovoltampere rating and other parameters of a 12-pulse delta connected ATRU were deduced by using the different tap position of the secondary side winding as the variable. The authors discussed the effects of the secondary winding tap positions on the ATRU input and output performance. By the analysis in [18], the output voltage amplitude can drop to 26%, and it needed extended winding in the primary side to step-up the output voltage. However, the auto-transformer winding structure is more complex. The authors of [19] discussed the effects of changes in the output voltage vector phase-shift angle on the 12-pulse ATRU input and output performances and the kilovoltampere rating. It was proved that when phase-shift angle is increased to 90°, the 5th and 7th harmonics are eliminated and the output voltage can be increased by 1.414 times. The output voltage range is not adjustable and the kilovoltampere rating of the auto-transformer is increased. The authors of [20] studied the step-down and step-up 18-pulse ATRU. When compared with

Manuscript received Dec. 29, 2016; accepted Oct. 12, 2017
Recommended for publication by Associate Editor Trillion Q Zheng.
†Corresponding Author : 1585411776@qq.com
Tel: +86-18762407215, Nanjing Univ. of Aeronautics and Astronautics
*Nanjing University of Aeronautics and Astronautics, China

the traditional 18-pulse ATRU, the proposed structure can regulate output voltage by changing the input phase voltage terminal on auto-transformer. The voltage gain range of the DT-topology is 0.97-2, These two structures are main to step-up voltage, the range of step-down is very small.

This paper puts forward a new step-down and step-up 12-pulse ATRU topology. There are two middle taps in each primary winding and connect to other two phase secondary windings. The auto-transformer output voltage vector is formed by part of the primary voltage vectors and secondary voltage vectors. By reasonably designing the middle tap positions and the dotted terminals of auto-transformer winding, the value of ATRU output voltage can be changed when the number of windings changes. There is a wide output voltage range, which fundamentally solves the problem that ATRU output voltage is hard to regulate. Based on the proposed structure, the expressions for the ratio of winding, winding current and kilovoltampere rating are deduced. Furthermore, the total harmonic distortion of the input current and the change of kilovoltampere rating are analyzed. Finally, simulation and experiments are carried out to verify the feasibility of the design.

II. Topology of the Step-Up and Step-Down ATRU

A. Winding Connection

This paper presents a new topology of the step-up and step-down ATRU, which is shown in Fig. 1. The structure of auto-transformer winding is based on the delta connection. The features of this winding connection are explained as follows. 1) The delta structure is composed of primary three phase winding: ab, bc and ca. The numbers of these winding are equal. 2) There are 2 middle taps in each primary windings. For example, a_1 and a_2 are the middle taps of A phase (winding ab) connected to the secondary winding of C phase and B phase, respectively. In addition, the connection of B phase and C phase primary windings are similar to A phase as shown in Fig. 1. 3) There are 2 secondary windings in each phase. The number of secondary windings is equal. The output terminals of auto-transformer are a', b', c' and a", b", c", which connect to the input terminals of bridge rectifier 1 and bridge rectifier 2 respectively. 4) The other terminals of the secondary side are a_1, a_2, b_1, b_2, c_1 and c_2, which are connected to the corresponding middle taps of primary winding. 5) The auto-transformer output voltages are related to the change of the dotted terminals of the secondary winding. The change of dotted terminals are shown in Fig. 1. When "▪" is chosen as the dotted terminal this is called working mode 1; and when "△" is chosen as the dotted terminal this is called working mode 2. Working modes 1 and 2 can be selected by changing the dotted terminal of auto-transformer windings. Working modes 1 and 2 have

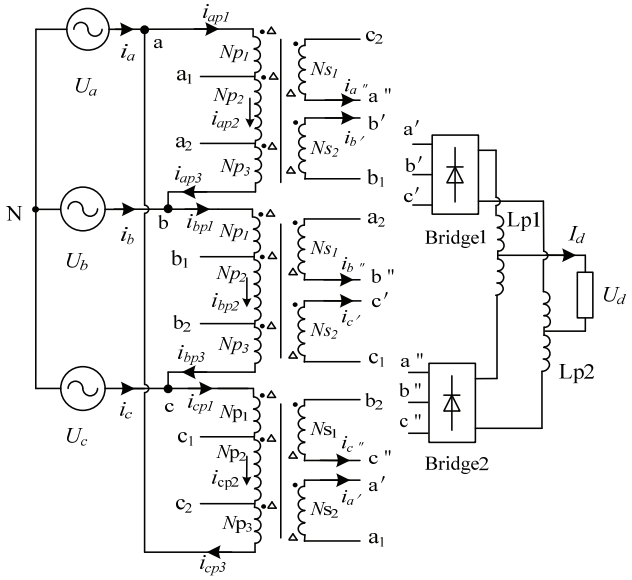

Fig. 1. Topology of step-down and step-up 12 pulse ATRU.

their respective ranges of voltage regulation. Thus, the ATRU can output different voltage amplitudes with dotted terminal changes and different ratios of windings.

B. Vector of the Transformer Winding Voltage

According to the winding connection in Fig. 1, the auto-transformer voltage vector is related to the dotted terminal and the ratio of winding. Fig. 2(a) shows the auto-transformer winding voltage vector of working mode 1; and Fig. 2 (b) shows auto-transformer winding voltage vector of working mode 2. The labels in Fig. 2 (a) and Fig. 2 (b) correspond to the labels in Fig. 1. The voltage vectors correspond to the windings on the same phase are in the same direction or reverse. U_{aN}, U_{bN}, U_{cN} are input phase voltage. $U_{a'N}$, $U_{b'N}$, $U_{c'N}$ and $U_{a''N}$, $U_{b''N}$, $U_{c''N}$ are two groups of three phase output voltage where the amplitudes are equal. In order to ensure the elimination of the 5th and 7th harmonics in a 12-pulse rectifier, two groups of output voltages need to satisfy a certain phase-shift angle. α is the angle between the output phase voltage vector and the input voltage vector, N is the number of rectifier bridges in system. The relationship between α and N is [5]:

$$2\alpha = \frac{60°}{N} \tag{1}$$

As shown in Fig. 1, N is 2, and the calculated α is equal to 15°. Thus, voltage phase of $U_{a'N}$, $U_{b'N}$, $U_{c'N}$ lag input three-phase voltage by 15°; the voltage phase of $U_{a''N}$, $U_{b''N}$, $U_{c''N}$ advanced input three-phase voltage by 15°; and the phase difference between two groups of output voltage is 30°. These voltage parallel outputs flow across two rectifier bridges and the inter-phase reactor.

The following subsection will explain the ratio of winding and the output voltage vector synthesis. Taking A phase as an example, assuming that the total number of primary windings ab is N_p, which divides the two middle taps (a1, a2) into

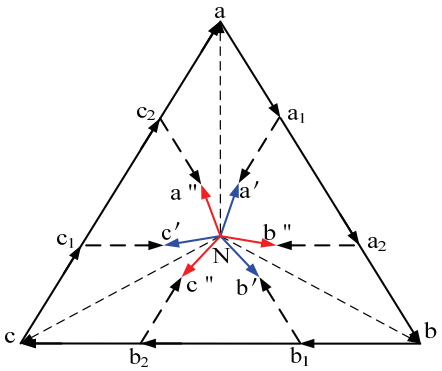

Fig. 2(a). Vector diagram of auto-transformer winding voltage of working mode 1.

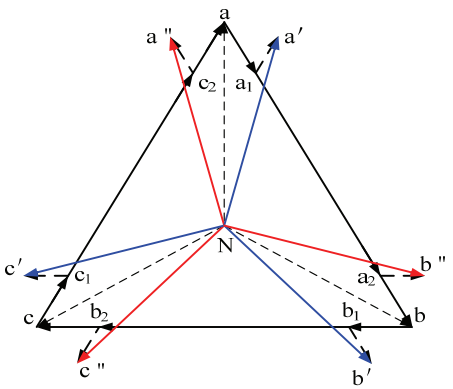

Fig. 2(b). Vector diagram of auto-transformer winding voltage of working mode 2.

three sections (aa_1, a_1a_2, a_2b). In addition, the number of windings aa_1, a_1a_2 and a_2b are N_{p1}, N_{p2} and N_{p3} respectively ($N_p = N_{p1} + N_{p2} + N_{p3}$); the number of secondary winding c_2a'' and $b'b_1$ are N_{s1} and N_{s2} ($N_{s1} = N_{s2}$). Define the ratio of windings K_{p1}, K_{p2}, K_{p3}, K_{s1} and K_{s2} as follows:

$$\begin{cases} K_{p1} = K_{p3} = N_{p1}/N_p = N_{p3}/N_p \\ K_{p2} = N_{p2}/N_p \\ K_{s1} = K_{s2} = N_{s1}/N_p = N_{s2}/N_p \end{cases} \tag{2}$$

As shown in Fig. 2(a) and Fig. 2(b), the output phase voltage vectors of the auto transformer can be derived. Taking $\dot{U}_{a'N}$ and $\dot{U}_{a''N}$ as examples:

$$\begin{cases} \dot{U}_{a'N} = \dot{U}_{aN} + \dot{U}_{a1a} + \dot{U}_{a'a1} = \dot{U}_{aN} + K_{p1}\dot{U}_{ba} - K_{s2}\dot{U}_{ac} \\ \dot{U}_{a''N} = \dot{U}_{c2c} + \dot{U}_{a''c2} = (K_{p1} + K_{p2})\dot{U}_{ac} + K_{s1}\dot{U}_{ba} \end{cases} \tag{3}$$

In B phase and C phase, the number of wingdings are similar to A phase and the rest of output voltage vector expressions are similar to Equation (3).

C. Structural Improvement and Innovation

When compared to earlier references in the area of auto-transformer tapping designs[17,18,20], the winding connection is different in this paper. For ease of illustration, the labels in Fig. 1 and Fig. 2 are still used. Delta-connected structures are also proposed in [17] and [18]. Taking the winding ac as an example, the middle tap c_1 is connected to the secondary winding c_2a'', and c_2a'' is wound with the winding bc in the same phase. When output voltage $\dot{U}_{a''N}$ is formed, the voltage vectors $\dot{U}_{a''c2}$ and $\dot{U}_{bc}$ are paralleled. However, in this paper, the winding c_2a'' is wound with the winding ab in the same phase. Therefore, when output voltage $U_{a''N}$ is formed, the voltage vectors $\dot{U}_{a''c2}$ and $\dot{U}_{ba}$ are reversed. Therefore, the winding voltage vectors involved in the output voltage synthesis are different, and the corresponding ratio of windings is different. Furthermore, when the positions of middle taps are changed, for example a_1 coincidence with point a, the connection mode shown in Fig. 1 gives a wider range of output voltage.

The 18 pulse ATRU is discussed in [20], and the proposed scheme also adds middle taps in the autotransformer. However, these middle taps are connected to the input three-phase voltage. The shift of middle tap changes the length and direction of the input voltage vector. In this way, the winding voltage vectors are unchanged. However, the output voltage can be regulated by changing input voltage vector. In this paper, the input voltage vector is constant but winding voltage vectors are varied. From the results obtained, the voltage regulation of the proposed scheme in [20] is smaller.

III. Voltage Ratio and Ratio of Winding

A. Ratio of Auto-Transformer Winding

In order to make the phase angle and amplitude of the output voltage vector satisfy a certain relation, the ratio of auto-transformer winding should be reasonable designed, and it can be deduced by voltage vector diagram. With A phase as a reference, assume that the input and output line voltage effective values of the auto-transformer are V_i and V_o respectively, and that K_u is the voltage ratio of auto-transformer, which is equal to V_i/V_o. The ratio of winding expressions are deduced while the voltage ratio K_u is uses as a parameter.

In the situation of auto-transformer working mode 1, the output voltage vector of the auto-transformer $U_{a'N}$ is shown in Fig. 3(a). To simplify the calculation, assume the segment length to be $aN = 1$. Thus, $a'N = K_u$. In the triangle Naa', according to the cosine theorem, aa' and $\angle Naa'$ can be solved by equations (4) and (5):

$$\begin{aligned} aa' &= \sqrt{1^2 + K_u^{\,2} - 2\times 1\times K_u \times \cos 15^\circ} \\ &= \sqrt{K_u^{\,2} + 1 - 1.932K_u} \end{aligned} \tag{4}$$

$$\angle Naa' = \arccos\left(\frac{2 - 1.932K_u}{2\sqrt{K_u^{\,2} + 1 - 1.932K_u}}\right) \tag{5}$$

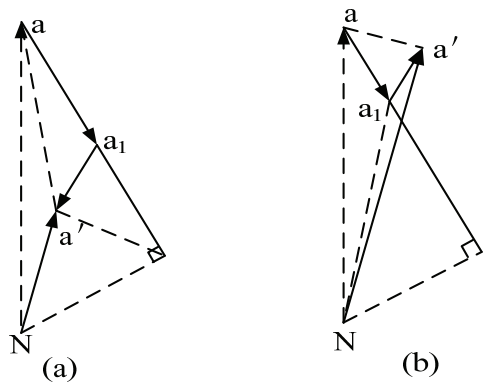

Fig. 3. Vector diagrams of output voltage $U_{a'N}$.

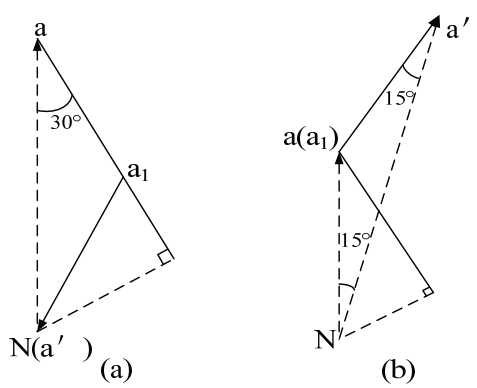

Fig. 4. Vector diagrams of $U_{a'N}$ in limiting cases.

In triangle $aa'a1$, $\angle aa1a'=120°$. According to the sine theorem and cosine theorem, the length of aa_1 and $a'a_1$ can be calculated by equations (6) and (7):

$$aa_1=\frac{\sqrt{3}}{2}\sqrt{K_u{}^2+1-1.932K_u}\times \sin(30°+\arccos(\frac{2-1.932K_u}{2\sqrt{K_u{}^2+1-1.932K_u}})) \tag{6}$$

$$a'a_1=\frac{\sqrt{3}}{2}\sqrt{K_u{}^2+1-1.932K_u}\times \sin(30°-\arccos(\frac{2-1.932K_u}{2\sqrt{K_u{}^2+1-1.932K_u}})) \tag{7}$$

According to equations (4)-(7), the ratio of winding expressions are deduced as shown in equations (8)-(10):

$$K_{p1}=K_{p3}=\frac{N_{p1}}{N_p}=\frac{\sqrt{K_u^2+1-1.932K_u}}{1.5}\times \sin(30°+\arccos(\frac{2-1.932K_u}{2\sqrt{K_u^2+1-1.932K_u}})) \tag{8}$$

$$K_{p2}=\frac{N_{p2}}{N_p}=1-2K_{p1} \tag{9}$$

$$K_{s1}=K_{s2}=\frac{N_{s1}}{N_p}=\frac{\sqrt{K_u^2+1-1.932K_u}}{1.5}\times \sin(30°-\arccos(\frac{2-1.932K_u}{2\sqrt{K_u^2+1-1.932K_u}})) \tag{10}$$

Similarly, it can deduce the ratio of the winding expressions in the case of working mode 2. In this situation, the change of the secondary side voltage vector direction is caused by the change of secondary winding dotted terminals. The ratio of primary winding expressions (K_{p1}, K_{p2}, K_{p3}) are unchanged, just same as equations (8) and (9), the ratio of secondary winding expression is changed as equation. (11):

$$K_{s1}=K_{s2}=\frac{N_{s1}}{N_p}=\frac{\sqrt{K_u^2+1-1.932K_u}}{1.5}\times \left|\sin(30°-\arccos(\frac{2-1.932K_u}{2\sqrt{K_u^2+1-1.932K_u}}))\right| \tag{11}$$

In summary, the ratio of primary winding can be solved by equations (8) and (9), and the ratio of secondary winding can be solved by equation (11) in the both two working modes of the auto-transformer.

B. Range of Auto-Transformer Output Voltage

In this paper, the range of auto-transformer output voltage is related to the ratio of winding and dotted terminals. According to the two working mode voltage vector diagrams and equations (8)-(11), the output voltage amplitude limit of auto-transformer can be solved. Taking the same output voltage $U_{a'N}$ as an example.

Fig. 4(a) shows the situation of minimum output voltage. In this situation, a' coincidence with the neutral point N. In triangle $aa'a_1$, $aa_1=a_1a'$ and $\angle aa_1a'=120°$. Then, it can be solved that $aa_1=a_1a'=aN/\sqrt{3}=ab/3$. Furthermore, the ratio of primary winding can be calculated as: $K_{p1}=K_{p2}=K_{p3}=1/3$. Thus, the minimum voltage ratio of the auto-transformer is 0.

Fig. 4(b) shows the situation of maximum auto-transformer output voltage. This can be obtained when the middle tap a_1 coincidence with point a. In this situation $K_{p1}=0$. By bringing $K_{p1}=0$ into equation (8), the maximum voltage ratio is calculated as 1.932 .

In summary, the range of K_u is 0-1.932. Some typical values of K_u and the ratios of windings are shown in table I. When K_u is 0.707, the number of secondary windings is 0, and the change of ATRU working mode takes this situation as a critical point. In addition, the auto-transformer only contains three-phase primary winding, and the middle taps of

TABLE I
TYPICAL VOLTAGE RATIOS AND RATIOS OF THE WINDINGS

K_u	0.5	0.707	1.0	1.2	1.932
K_p、K_{p3}	0.247	0.211	0.161	0.126	0
K_{p2}	0.506	0.578	0.678	0.748	1
K_{s1}、K_{s2}	0.098	0	0.138	0.232	0.577

primary winding are the output terminals of auto-transformer. This is the simplest auto-transformer structure. When K_u is 1.932, there are no middle taps in primary winding, auto-transformer output voltage is the maximum value.

IV. ANALYSIS OF INPUT AND OUTPUT CURRENT

The auto-transformer winding configuration of working mode 1 is shown in Fig. 5. With the current through winding, which is shown in Fig. 1, according to the principle of magnetic potential balance and Kirchhoff's current law, the nodal current equation and magnetic circuit equation of each iron core column can be listed as equations (12) and (13):

$$\begin{cases} N_{p1}(i_{a'}+i_{cp3}+i_{b''})+N_{p2}(i_2+i_{b''})+N_{p3}(i_2)=N_{s1}i_{b'}-N_{s2}i_{a''} \\ N_{p1}(i_{b'}+i_{ap3}+i_{c''})+N_{p2}(i_3+i_{c''})+N_{p3}(i_3)=N_{s1}i_{c'}-N_{s2}i_{b''} \\ N_{p1}(i_{c'}+i_{bp3}+i_{a''})+N_{p2}(i_1+i_{a''})+N_{p3}(i_1)=N_{s1}i_{a'}-N_{s2}i_{c''} \end{cases} \quad (12)$$

$$\begin{cases} i_a+i_{cp3}=i_{b''}+i_{a'}+i_2 \\ i_b+i_{ap3}=i_{c''}+i_{b'}+i_3 \\ i_c+i_{bp3}=i_{a''}+i_{c'}+i_1 \end{cases} \quad (13)$$

The input currents of auto-transformer can be solved from Equs. (12)-(13). Taking A phase as an example, the input current i_a is expressed as follow:

$$\begin{aligned} i_a=&\left(K_{p1}+K_{p2}-K_{s1}\right)i_{a'}+\left(K_{p1}+K_{p2}-K_{s1}\right)i_{a''} \\ &+K_{s1}i_{b'}+K_{p1}i_{b''}+K_{p1}i_{c'}+K_{s1}i_{c''} \end{aligned} \quad (14)$$

Because of two groups of output voltages are paralleled, two rectifier bridges working at the same time, each rectifier bridges through half of the output current and diode conduct 120° in each cycle. Assuming ATRU output current is I_d, by introducing I_d into Equ. (14) to obtain Equ. (15). The diagram of input current I_a is symmetric 12 step wave which is shown in Fig. 6.

$$I_a=\begin{cases} \frac{1}{2}\left(K_{p1}+K_{p2}-2K_{s1}\right)I_d, \omega t\in\left(0,\frac{\pi}{6}\right) \\ \frac{1}{2}\left(K_{p1}+2K_{p2}-3K_{s1}\right)I_d, \omega t\in\left(\frac{\pi}{6},\frac{\pi}{3}\right) \\ \left(K_{p1}+K_{p2}-2K_{s1}\right)I_d, \omega t\in\left(\frac{\pi}{3},\frac{\pi}{2}\right) \end{cases} \quad (15)$$

It can be obtained from the Fourier decomposition of input current I_a:

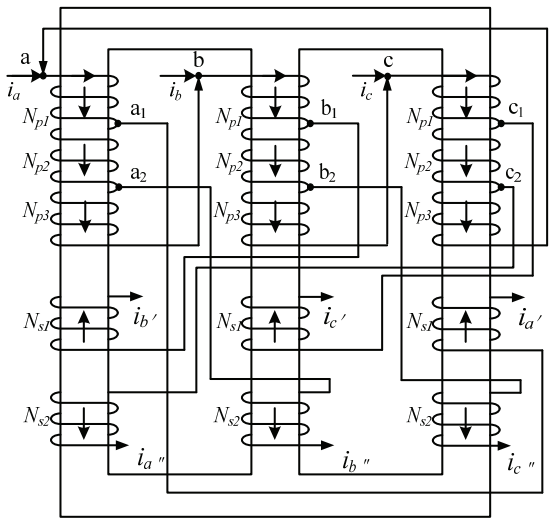

Fig. 5. Auto-transformer winding configuration of working mode 1.

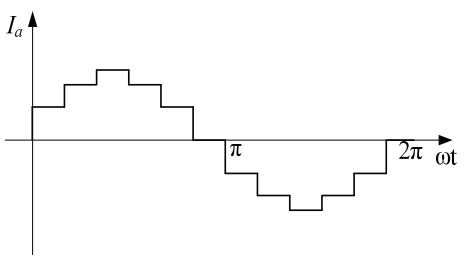

Fig. 6. Diagram of input current I_a.

$$I_a=\frac{2I_d}{\pi}\sum_{n=1,11,13\cdots}^{\infty}\frac{1}{n}\begin{bmatrix}\left(K_{p1}+K_{p2}-2K_{s1}\right)\cos\frac{n\pi}{12} \\ +\left(K_{p2}-K_{s1}\right)\cos\frac{3n\pi}{12} \\ +\left(K_{p1}-K_{s1}\right)\cos\frac{5n\pi}{12}\end{bmatrix}\sin n\omega t \quad (16)$$

Auto-transformer winding configuration of working mode 2 is shown in Fig. 7. The current direction that flows through the winding is unchanged so that nodal current equations are not changed just as Equ. (13). However, dotted terminals of secondary winding are different from working mode 1, this causes magnetic circuit equations changed as Equ. (17):

$$\begin{cases} N_{p1}(i_{a'}+i_{cp3}+i_{b''})+N_{p2}(i_2+i_{b''})+N_{p3}i_2=-N_{s1}i_{b'}+N_{s2}i_{a''} \\ N_{p1}(i_{b'}+i_{ap3}+i_{c''})+N_{p2}(i_3+i_{c''})+N_{p3}i_3=-N_{s1}i_{c'}+N_{s2}i_{b''} \\ N_{p1}(i_{c'}+i_{bp3}+i_{a''})+N_{p2}(i_1+i_{a''})+N_{p3}i_1=-N_{s1}i_{a'}+N_{s2}i_{c''} \end{cases} \quad (17)$$

Input current i_a is solved as follows:

$$\begin{aligned} i_a=&\left(K_{p1}+K_{p2}+K_{s1}\right)i_{a'}+\left(K_{p1}+K_{p2}+K_{s1}\right)i_{a''} \\ &-K_{s1}i_{b'}+K_{p1}i_{b''}+K_{p1}i_{c'}-K_{s1}i_{c''} \end{aligned} \quad (18)$$

In this situation, the input current is still a symmetric 12 step wave which is similar to Fig. 6. But the amplitude is changed as follows:

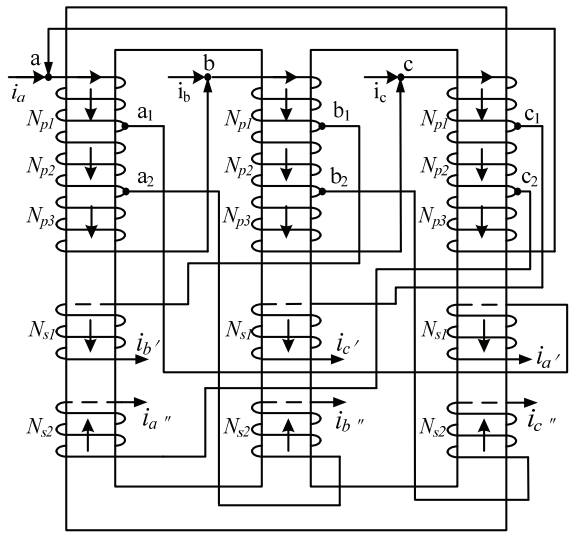

Fig. 7. Auto-transformer winding configuration of working mode 2.

$$I_a=\begin{cases}\frac{1}{2}\left(K_{p1}+K_{p2}+2K_{s1}\right)I_d, \omega t\in\left(0,\frac{\pi}{6}\right)\\ \frac{1}{2}\left(K_{p1}+2K_{p2}+3K_{s1}\right)I_d, \omega t\in\left(\frac{\pi}{6},\frac{\pi}{3}\right)\\ \left(K_{p1}+K_{p2}+2K_{s1}\right)I_d, \omega t\in\left(\frac{\pi}{3},\frac{\pi}{2}\right)\end{cases} \tag{19}$$

Fourier decomposition of the Equ. (19), it can be obtained that:

$$I_a=\frac{2I_d}{\pi}\sum_{n=1,11,13\cdots}^{\infty}\frac{1}{n}\begin{bmatrix}\left(K_{p1}+K_{p2}+2K_{s1}\right)\cos\frac{n\pi}{12}\\ +\left(K_{p2}+K_{s1}\right)\cos\frac{3n\pi}{12}\\ +\left(K_{p1}+K_{s1}\right)\cos\frac{5n\pi}{12}\end{bmatrix}\sin n\omega t \tag{20}$$

As Equ. (16) and Equ. (20) expressed, it can be concluded that in both two auto-transformer working modes, the input current only contains 12±1th harmonics and the lowest harmonic is the 11th. This result is consistent with the effect of the 12 pulse ATRU suppression harmonics mentioned in the references[7,9,12,16]. According to the expression $THD=\sqrt{\sum_{n=2}^{\infty}I_{sn}^2}\Big/I_{s1}$, the total harmonic distortion of the input current can be calculated.

V. KILOVOLTAMPERE RATING OF AUTO-TRANSFORMER

The formula to calculate the kilovoltampere rating of the auto-transformer is $P_{dtr}=0.5\sum\left(V_{rms}\times I_{rms}\right)$. V_{rms}, I_{rms} are effective value of voltage across and current through each winding. Define kilovoltampere rating ratio C_p is ratio of auto-transformer kilovoltampere rating to ATRU output power P_0; V_d and I_d are ATRU output DC voltage and current respectively, so C_p can be expressed as follows:

$$C_p=\frac{P_{dtr}}{P_0}=\frac{P_{dtr}}{V_dI_d} \tag{21}$$

Because of symmetry,the kilovoltampere rating of each phase are equal. Taking A phase as an example, assume effective value of voltage across and current through the primary winding are V_{p1}, V_{p2}, V_{p3} and I_{p1}, I_{p2}, I_{p3} respectively, these value corresponding to the primary winding which the number of winding are N_{p1}, N_{p2}, N_{p3} respectively; I_s and V_s are effective value of voltage across and current through the secondary winding; V_i is the effective value of input line voltage. It can be known that 12-pulse delta-connected ATRU output voltage is $V_{d'}$:

$$V_d'=\frac{1.35V_i}{\cos 15°} \tag{22}$$

Considering the voltage ratio K_u, the value of output DC voltage of step-up and step-down 12-pulse ATRU is :

$$V_d=1.35K_uV_i \tag{23}$$

The effective value of voltage across each winding are expressed as follows:

$$\begin{cases}V_{p1}=K_{p1}V_i\\ V_{p2}=K_{p2}V_i\\ V_{p3}=K_{p3}V_i\\ V_s=K_{s1}V_i\end{cases} \tag{24}$$

In both working mode 1 and mode 2, each rectifier bridge take half of the output current and diode conduct 120° in each cycle, so the expression of secondary winding current effective value is same and expressed in Equ. (25):

$$I_s=\sqrt{\frac{1}{\pi}\times\frac{8\pi}{12}\times\left(\frac{I_d}{2}\right)^2}=\frac{\sqrt{6}}{6}I_d \tag{25}$$

In the situation of working mode 1, the current relationships between A phase primary winding are expressed in Equ. (26).

$$\begin{cases}i_{ap1}=i_a+i_{cp3}\\ i_{ap2}=i_{ap1}-i_{a'}\\ i_{ap3}=i_{ap2}-i_{b''}\end{cases} \tag{26}$$

In combination with Equs. (12)-(13), the current through each primary winding can be calculated.

$$\begin{cases}i_{ap1}=\left(K_{p1}+K_{p2}\right)i_{a'}-K_{s2}i_{a''}+K_{s1}i_{b'}+K_{p1}i_{b''}\\ i_{ap2}=-K_{p1}i_{a'}-K_{s2}i_{a''}+K_{s1}i_{b'}+K_{p1}i_{b''}\\ i_{ap3}=-K_{p1}i_{a'}-K_{s2}i_{a''}+K_{s1}i_{b'}-\left(K_{p1}+K_{p2}\right)i_{b''}\end{cases} \tag{27}$$

The effective value of current through primary winding can be calculated by bringing ATRU output DC current I_d into Equ. (27):

$$\begin{cases} I_{p1}=\dfrac{I_d}{2\sqrt{6}}\sqrt{1+4K_{p1}{}^2+3K_{p2}{}^2+14K_{s1}{}^2+4K_{p1}K_{p2}-10K_{p2}K_{s1}} \\ I_{p2}=\dfrac{I_d}{2\sqrt{6}}\sqrt{8K_{p1}{}^2+14K_{s1}{}^2+20K_{p1}K_{s1}} \\ I_{p3}=\dfrac{I_d}{2\sqrt{6}}\sqrt{8K_{p1}{}^2+4K_{p2}{}^2+14K_{s1}{}^2+8K_{p1}K_{p2}-10K_{p2}K_{s1}} \end{cases} \quad (28)$$

According to Equs. (23)-(28), the expression of kilovoltampere rating is expressed as follows:

$$\begin{aligned} P_{dtr} &= \left[3(I_{p1}V_{p1}+I_{p2}V_{p2}+I_{p3}V_{p3})+6I_sV_s\right]\times 0.5 \\ &= \frac{V_d}{2.7K_u}\left[\sqrt{6}K_{s1}I_d+3K_{p1}I_{p1}+3K_{p2}I_{p2}+3K_{p1}I_{p3}\right] \end{aligned} \quad (29)$$

In the situation of working mode 2, the expression of kilovoltampere rating can be deduced just same as Equ. (29). However, in this case the current through primary winding is different from working mode 1 due to the change of dotted terminal, which can be expressed in Equ. (30).

$$\begin{cases} i_{ap1}=\left(K_{p1}+K_{p2}\right)i_{a'}+K_{s2}i_{a''}-K_{s1}i_{b'}+K_{p1}i_{b''} \\ i_{ap2}=-K_{p1}i_{a'}+K_{s2}i_{a''}-K_{s1}i_{b'}+K_{p1}i_{b''} \\ i_{ap3}=-K_{p1}i_{a'}+K_{s2}i_{a''}-K_{s1}i_{b'}-\left(K_{p1}+K_{p2}\right)i_{b''} \end{cases} \quad (30)$$

Also, the expressions of current effective value are changed as follows:

$$\begin{cases} I_{p1}=\dfrac{I_d}{2\sqrt{6}}\sqrt{1+4K_{p1}{}^2+3K_{p2}{}^2+14K_{s1}{}^2+4K_{p1}K_{p2}+10K_{p2}K_{s1}} \\ I_{p2}=\dfrac{I_d}{2\sqrt{6}}\sqrt{8K_{p1}{}^2+14K_{s1}{}^2-20K_{p1}K_{s1}} \\ I_{p3}=\dfrac{I_d}{2\sqrt{6}}\sqrt{8K_{p1}{}^2+4K_{p2}{}^2+14K_{s1}{}^2+8K_{p1}K_{p2}+10K_{p2}K_{s1}} \end{cases} \quad (31)$$

So, the kilovoltampere rating ratio C_p can be calculated by voltage ratio K_u. Table II shows some value of C_p with different K_u. Fig. 8 shows the relation curve between C_p and K_u.

According to Fig. 8 and the calculation, with the voltage ratio increased, the kilovoltampere rating ratio decreased and then increased:

(1) When K_u is 0.41, C_p is 1, and C_p is less than 1 when K_u is greater than 0.41. When the auto-transformer kilovoltampere rating ratio is greater than 1, there is no advantage when compared to the isolated transformer in terms of volume and weight. The proposed structure in this paper should not be used when voltage ratio is less than 0.41.

(2) When K_u is 0.707, auto-transformer structure without secondary winding, which is the simplest structure, in this situation C_p is 0.332.

(3) When K_u is 0.92, C_p is 0.292 which is the minimum value. After that C_p increased with the rise of K_u. When K_u reaches the maximum value of 1.932, C_p is 0.688.

(4) Under the condition of a wide output voltage range, to ensure a smaller volume and weight of the ATRU (C_p is less than 0.5), the range of K_u is about 0.61-1.86.

TABLE II
KILOVOLTAMPERE RATING RATIO C_p WITH DIFFERENT VALUES OF K_u

K_u	0.5	0.707	0.9	1.2	1.5	1.932
C_p	0.747	0.332	0.294	0.365	0.446	0.688

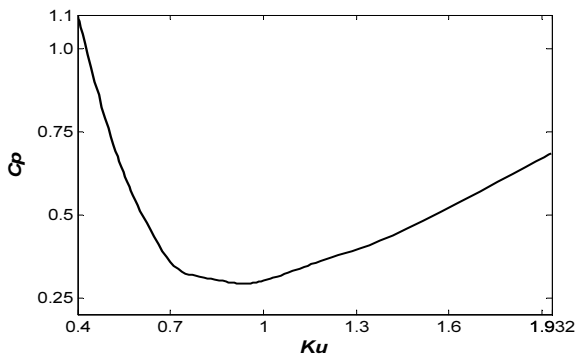

Fig. 8. Relationship between kilovoltampere rating ratio C_p and voltage ratio K_u.

VI. SIMULATION ANALYSIS AND EXPERIMENT

In order to verify the correctness of the analysis, the 12-pulse step-up and step-down ATRU is simulated in the Saber environment. In the situation of working mode 1, take $K_u=0.5$ as an example; in the situation of working mode 2, take $K_u=0.5$ and $K_u=1.2$ as examples. Each of the simulations is carries out under the condition of a three-phase AC input voltage (115V/400Hz) and a load of 1Ω.

When $K_u=0.5$, the auto-transformer output line voltage is shown in Fig. 9, and the effective value is 99.50V. Fig. 9(a) shows waveforms of $U_{a'c'}$ and $U_{a''c''}$. The phase difference time between $U_{a'c'}$ and $U_{a''c''}$ is 208.45μs. This time converted into its corresponding lag angle is 29.952°, which is in agreement with the theoretical value of 30°. Fig. 9(b) and Fig. 9(c) show two groups of three-phase output voltages. Fig. 10 shows the ATRU output DC voltage, which has an effective value of 133.84V, there are 12 pulse in a cycle. Fig. 11 shows the voltage across and the current through A phase winding. By measuring the effective value of the voltage and current, the kilovoltampere rating of A phase can be calculated. Because the kilovoltampere rating of B phase and C phase are equal to A phase, C_p can be calculated at 0.749, which is in agreement with the theoretical value of 0.747.

When $K_u=0.9$, the auto-transformer output line voltage is shown in Fig. 12, and its effective value is 179.68V. Fig. 12(a) are waveforms of $U_{a'c'}$ and $U_{a''c''}$, and the lag angle between them is about 30°. Fig. 12(b) and Fig. 12(c) show two groups three-phase output voltages. Fig. 13 shows the output DC voltage which effective value is 242.24V. Fig. 14

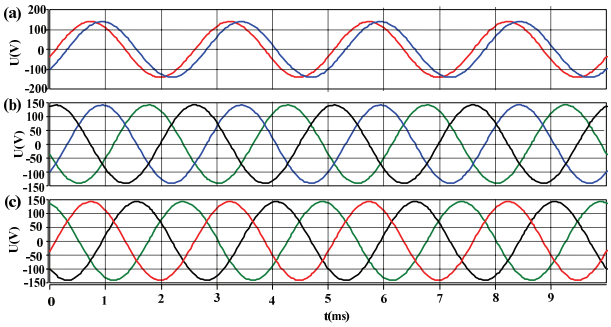

Fig. 9. Output line voltage of auto-transformer (K_u=0.5, Simulation).

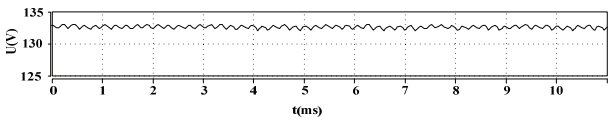

Fig. 10. Output DC voltage (K_u=0.5, Simulation).

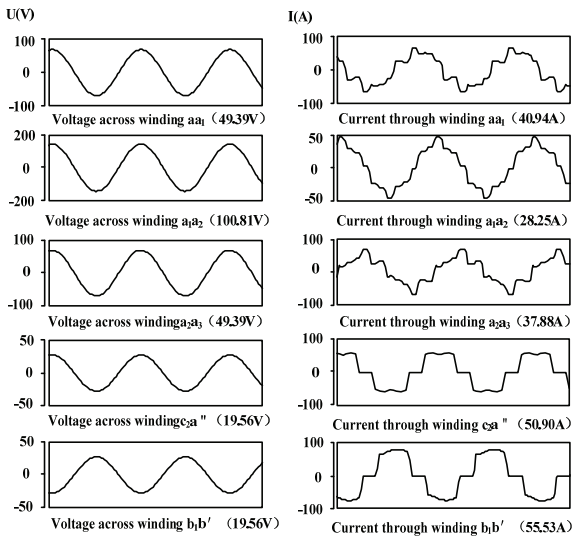

Fig. 11. Voltage and current through A phase winding (K_u=0.5, Simulation).

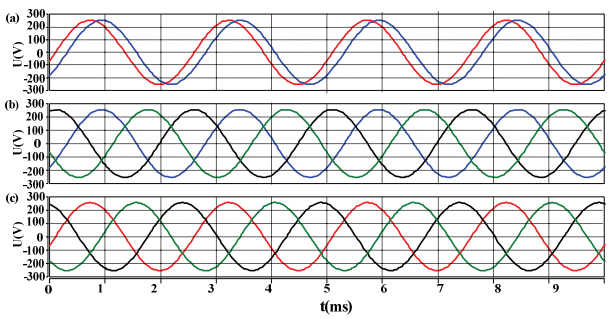

Fig. 12. Output line voltage of auto-transformer (K_u=0.9, Simulation).

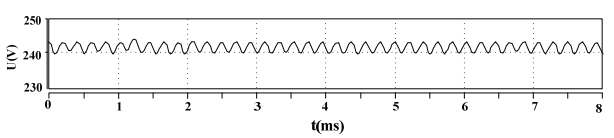

Fig. 13. Output DC voltage (K_u=0.9, Simulation).

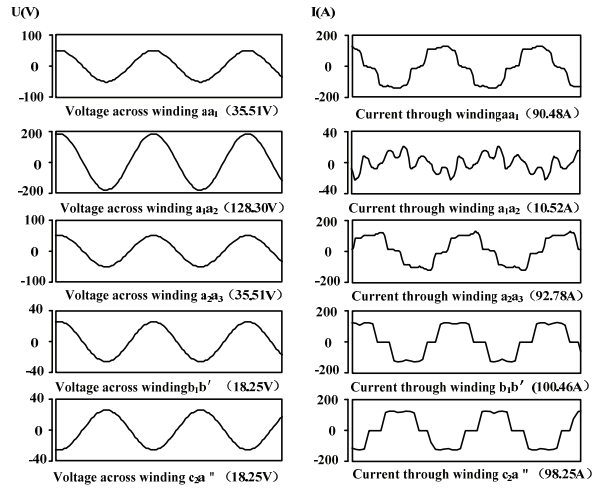

Fig. 14. Voltage and current through A phase winding (K_u=0.9, Simulation).

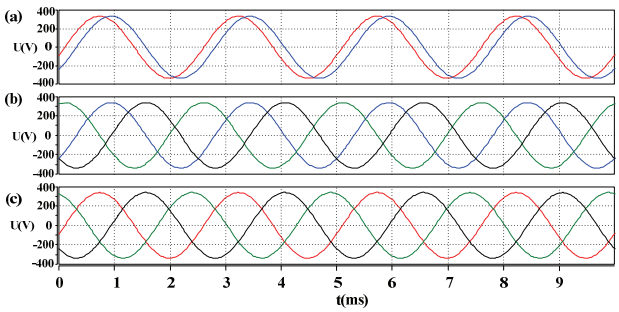

Fig. 15. Output line voltage of auto-transformer (K_u=1.2, Simulation).

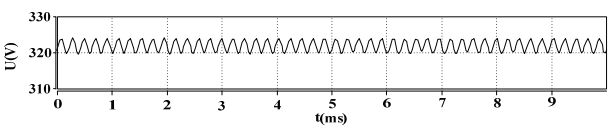

Fig. 16. Output DC voltage (K_u=1.2, Simulation).

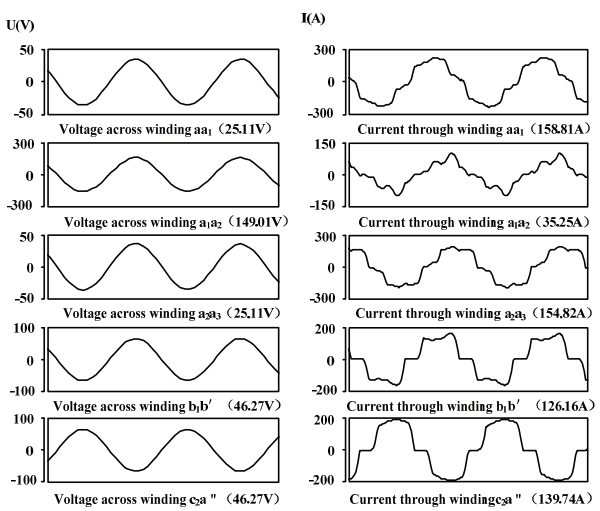

Fig. 17. Voltage and current through A phase winding (K_u=1.2, Simulation).

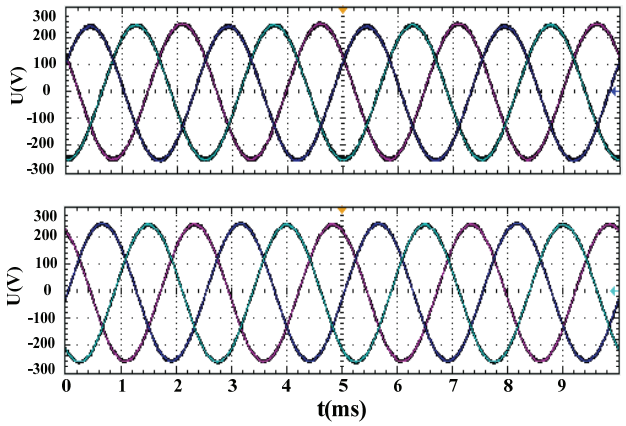

Fig. 18. Secondary side output three-phase line voltage of transformer (K_u=0.9, Experiment).

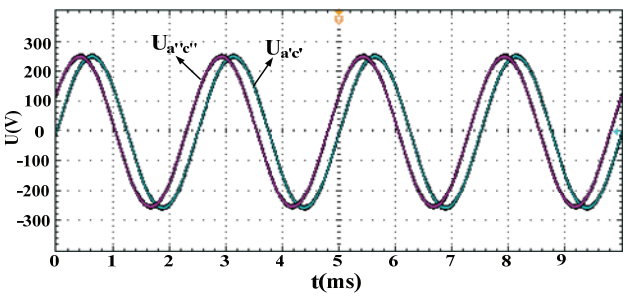

Fig. 19. Secondary side output line voltage of transformer (K_u=0.9, Experiment).

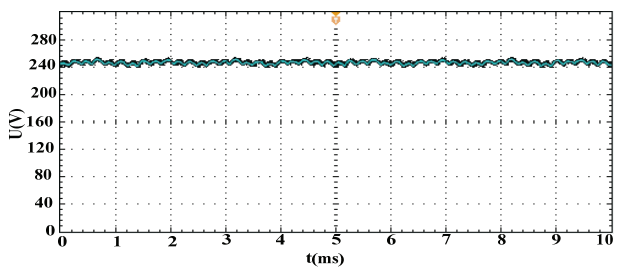

Fig. 20. Output DC voltage (K_u=0.9, Experiment).

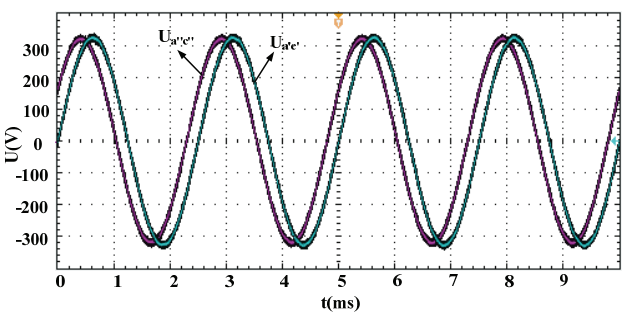

Fig. 21. Secondary side output line voltage of transformer (K_u=1.2, Experiment).

shows the voltage across and the current through A phase winding, and the calculated value of C_p is 0.296, which is in agreement with the theoretical value of 0.295.

When $K_u = 1.2$, the auto-transformer output line voltage

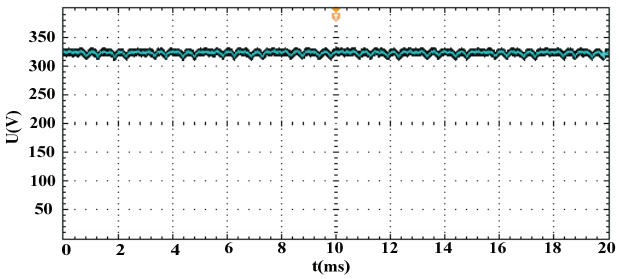

Fig. 22. Output DC voltage (K_u=1.2，Experiment).

is shown in Fig. 15, and the effective value is 179.68V. Fig. 15(a) shows waveforms of $U_{a'c'}$ and $U_{a''c''}$, and the lag angle between them is about 30°. Fig. 15(b) and Fig. 15(c) shows two groups of three-phase output voltages. Fig.16 shows the output DC voltage which effective value is 323.21V. Fig. 17 shows the voltage across and the current through A phase winding, and C_p is 0.367, which is in agreement with the theoretical value of 0.365.

In this paper, the new topology 12-pulse step-up and step-down ATRU with voltage ratios of 0.9 and 1.2 was designed and made. The input three-phase voltage is 115V/400Hz.

When K_u is 0.9, two groups of auto-transformer output line voltages are shown in Fig. 18, and the effective value of the line voltage is 179.6V. $U_{a'c'}$ and $U_{a''c''}$ are shown in Fig. 19, and the difference between two line voltage is about 0.21ms. The ATRU output DC voltage is 241.9V which shown in Fig. 20.

When K_u is 1.2, the effective value of line voltage is 238.7V. $U_{a'c'}$ and $U_{a''c''}$ are shown in Fig. 21, and the difference between two line voltages is about 0.21ms. The ATRU output DC voltage is 331.7V, which is shown in Fig. 22. The experimental results agree with the simulation analysis.

VII. CONCLUSION

This paper presents a new step-up and step-down multi-pulse auto-transformer rectifier structure. This structure can achieve a wide range of output voltages, which solves the problem of the auto-transformer output voltage being difficult to regulate. To achieve a wide range of output voltages, two working modes and the corresponding voltage vectors are determined. By using the voltage ratio of auto-transformer as a parameter, the relational expressions between the voltage ratio of auto-transformer, the ratio of winding, the input current and auto-transformer kilovoltampere rating in two working modes are deduced and summarized. According to these expressions, the effects of different voltage ratios on variation in the

kilovoltampere rating are discussed. The minimum value of kilovoltampere rating ratio is 0.292, and the optimized output voltage gain range is about 0.61-1.86, which can effectively reduce the weight and cost of the auto-transformer. By simulations and experiments of 12-pulse ATRU with two different voltage ratios, the correctness and practicability of the proposed structure are verified. According to the analysis of the 12 pulse ATRU proposed in this paper, the new structure can be applied to aviation and industrial applications. In recent experiments, it has been tested to supply a storage battery (220V) and a DC-DC convertor (output 28V). The analysis method used in this paper can also be used in the analysis of other ATRU structures.

ACKNOWLEDGMENT

This paper is funded by the following fund: Fundation of Graduate Innovation Center in NUAA (Fund number kfjj20170709); The National Natural Science Foundation of China (Fund number U51737006).

REFERENCES

[1] C. A. Arbugeri, T. B. Lazzarin, and S. A. Mussa, "Six-phase active PWM rectifier with synchronous frame reference control," in *2016 18th European Conference on Power Electronics and Applications (EPE'16 ECCE Europe)*, Karlsruhe, pp. 1-6, 2016.

[2] V. M. Quang, H. Wei, W. Dazhi, and W. Xuming, "A new type of PWM rectifier with function of harmonic suppression and reactive power compensation," in *2013 25th Chinese Control and Decision Conference (CCDC)*, Guiyang, 2013, pp. 3013-3017.

[3] X. Liu, Q. Zhang, D. Hou, and S. Wang, "Improved spacevector modulation strategy for AC-DC matrix converters," *J. Power Electron.,* Vol. 13, No. 4, pp. 647-655, Jul. 2013.

[4] T. L. Van and D.-C. Lee, "Developing function models of back-to-back PWM converters for simplified simulation," *J. Power Electron.*, Vol. 11, No. 1, pp. 51-58, Sep. 2011.

[5] D. A. Paice, *Power Electronic Converter Harmonic Multipulse Methodsfor Clean Power*. New York: IEEE Press, 1996.

[6] S. Choi, P. N. Enjeti, and I. J. Pitel, "Polyphase transformer arrangements with reduced kVA capacities for harmonic current reduction in rectifier-type utility interface," *IEEE Trans. Power Electron.*, Vol. 11, No. 5, pp. 680-690, Sep. 1996.

[7] G. Gong, U. Drofenik, and J. W. Kolar, "12-pulse rectifier for more electric aircraft applications," *IEEE International Conference on Industrial Technology,* Vol. 2, pp. 1096-1101, 2003.

[8] B. Singh, S. Gairola, A. Chandra, and K. Al-Haddad, "Zigzag connected auto-transformer based controlled ac-dc converter for pulse multiplication," *2007 IEEE International Symposium on Industrial Electronics*, pp. 889-894, 2007.

[9] Reng. Z. X, "Research on multi-pulse auto-transformer rectifier units (ATRU)," M.S. Thesis, Nanjing University of Aeronautics & Astronautics, China, 2008.

[10] B. Singh, G. Bhuvaneswari, and V. Garg, "Harmonic mitigation using 12-pulse AC-DC converter in vector-controlled induction motor drives," *IEEE Trans. Power Del.*, Vol. 21, No. 3, pp. 1483-1492, July 2006.

[11] A. Uan-Zo-li, R. Burgos, F. Lacaux, A. Roshan, F. Wang, and D. Boroyevich, "Analysis of new step-up and step-down direct symmetric 18-pulse topologies for aircraft autotransformer-rectifier units," *Power Electronics Specialists Conference IEEE*, pp. 1142-1148, 2005.

[12] X. W. Xie, M. Wang, and F. H. Zhang, "12-pulse auto-transformer rectifier unit with current harmonic injection," *Power Electron.*, Vol. 45, No. 11, pp. 9-11, Nov. 2011.

[13] F. Meng, W. Yang, S. Yang, and L. Gao, "Active harmonic reduction for 12-pulse diode bridge rectifier at DC side with two-stage auxiliary circuit," *IEEE Trans. Ind. Informat.*, Vol. 11, No. 1, pp. 64-73, Feb. 2015.

[14] G. R. Kamath, B. Runyan and R. Wood, "A compact auto-transformer based 12-pulse rectifier circuit," *Industrial Electronics Society, 2001. IECON '01. The 27th Annual Conference of the IEEE*, Denver, CO, Vol. 2. pp. 1344-1349, 2001.

[15] B. S. Lee, Jaehong Hahn, P. N. Enjeti, and I. J. Pitel, "A robust three-phase active power-factor-correction and harmonic reduction scheme for high power," *IEEE Trans. Ind. Electron.*, Vol. 46, No. 3, pp. 483-494, Jun. 1999.

[16] K. Emadi and M. Ehsani, "Aircraft power systems: Technology, state of the art, and future trends," *IEEE Aerosp. Electron. Syst. Mag.,* Vol. 15, No. 1, pp. 28-32, Jan. 2000.

[17] R. C. Fernandes, P. da Silva Oliveira, and F. J. M. de Seixas, "A family of autoconnected transformers for 12- and 18-pulse converters – Generalization for delta and wye topologies," *IEEE Trans. Power Electron.*, Vol. 26, No. 7, pp. 2065-2078, Jul. 2011.

[18] F. Meng, W. Yang, and S. Yang, "Effect of voltage transformation ratio on the kilovoltampere rating of delta-connected auto-transformer for 12-pulse rectifier system," *IEEE Trans. Ind. Electron.*, Vol. 60, No. 9, pp. 3579-3588, Sep. 2013.

[19] L. Gao, W. M. Tong, and F. G. Meng, "12-pulse rectifier system based on a novel step-up autotransform," *Journal of Power Supply,* No. 3, pp. 23-31, May. 2012.

[20] R. P. Burgos, A. Uan-Zo-li, and F. Lacaux, "Analysis of new step-up and step-down 18-pulse direct asymmetric auto-transformer-rectifiers," *Fourtieth IAS Annual Meeting*, Vol. 1, pp. 145-152, 2005.

[21] S. Yang, F. Meng, and W. Yang, "Optimum design of interphase reactor with double-tap changer applied to multipulse diode rectifier," *IEEE Trans. Ind. Electron.*, Vol. 57, No. 9, pp. 3022-3029, Sep. 2010.

Fan Jiang was born in Jiangxi, China, in 1993. He received his B.S. degree in Electrical Engineering and Automation from the Nanjing University of Aeronautics and Astronautics (NUAA), Nanjing, China, in 2014, where he is presently working towards his M.S. degree in Civil Aviation Electrical Engineering. His current research interests include multi-pulse rectification technology and aviation power supplies.

Hong juan Ge was born in Jiangsu, China, in 1966. She received her B.S. and M.S. degrees in Electrical Engineering from Southeast University, Nanjing, China, in 1985 and 1988, respectively; and her Ph.D. degree in Electric Machines and Electric Apparatus from the Nanjing University of Aeronautics and Astronautics (NUAA), Nanjing, China, in 2006. Her current research interests include space-vector control of PWM, AC-AC converters, and airworthiness technology.

Xiaoxu Dong was born in Liaoning, China, in 1997. She is presently working towards her B.S. degree in Civil Aviation Electrical Engineering at the Nanjing University of Aeronautics and Astronautics (NUAA), Nanjing, China. Her current research interests include electrical engineering and airworthiness technology.

Lu Zhang was born in Jiangsu, China, in 1994. She received her B.S. degree in Aircraft Airworthiness Technology from the Nanjing University of Aeronautics and Astronautics (NUAA), Nanjing, China, in 2016, where she is presently working towards her M.S. degree in Airworthiness Technology and Management. Her current research interests include multi-pulse rectification technology and aviation power supplies.